inter•noise 96
25th Anniversary Congress – Liverpool
INCE: 46.2

STRUCTURE BORNE SOUND ENERGY FLOW THROUGH VIBRATION ISOLATORS

L Karl

MWL Department of Vehicle Engineering, Royal Institute of Technology, Sweden

1. INTRODUCTION

There are mainly three different methods to determine the structure borne sound energy flow through vibration isolators [1-11], see Fig. 1.

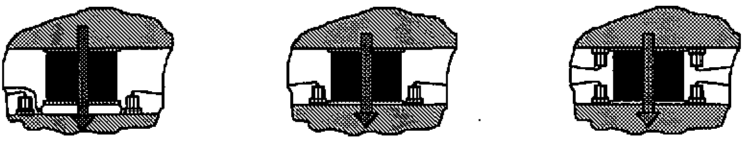

Method A Method B Method C

Figure 1. Three methods for measurement of energy flow through vibration isolators.

Method C has been developed and tested within this project.

2. THE METHOD

Theory

A useful representation of fields at junctions between isolator and mounting structures is by generalized variables acting at the center of the junctions. In Fig. 2, stress fields are represented by generalized force tensors and displacement fields are represented by generalized displacement tensors. Each generalized variable consists of six components. The technique is known as multi port method.

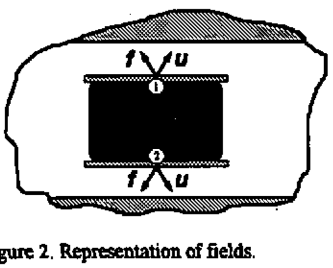

Figure 2. Representation of fields.

The time avaraged structure borne sound energy flow through a vibration isolator and induced into receiving structure is expressed by

$$\langle P \rangle = -\frac{1}{2\pi}\int_{-\infty}^{\infty} i\omega\, \boldsymbol{i} : \tilde{\boldsymbol{r}}(\tilde{\boldsymbol{f}}|_2, \tilde{\boldsymbol{u}}|_2)\, d\omega\,, \tag{1}$$

where i is imaginary unit, ω is angular frequency, $\boldsymbol{i}$ is second order unit tensor, $\tilde{\boldsymbol{r}}$ is second order spectrum density tensor, $:$ denotes double contraction and $\tilde{(\cdot)} = \int_{-\infty}^{\infty} (\cdot) e^{-i\omega t} dt$, is temporal Fourier transform. The correlation tensor is given by

$$\boldsymbol{r}(\boldsymbol{f}, \boldsymbol{u}) = \lim_{T\to\infty} \frac{1}{T} \int_{-T/2}^{T/2} \boldsymbol{f}(\tau) \otimes \boldsymbol{u}(\tau + t) d\tau\,, \tag{2}$$

where $\otimes$ is the classical tensor product. Through the relation

$$\tilde{\boldsymbol{f}}|_2 = \tilde{\boldsymbol{k}}_{12} \cdot \tilde{\boldsymbol{u}}|_1 + \tilde{\boldsymbol{k}}_{22} \cdot \tilde{\boldsymbol{u}}|_2\,, \tag{3}$$

where $\cdot$ denotes single contraction, $\tilde{\boldsymbol{k}}_{12}$ and $\tilde{\boldsymbol{k}}_{22}$ are second order dynamic transfer and driving point stiffness tensors, respectively, the relation (1) reads

$$\langle P \rangle = -\frac{1}{2\pi}\int_{-\infty}^{\infty} i\omega [\tilde{\boldsymbol{k}}_{12}^* : \tilde{\boldsymbol{r}}_{12} + \tilde{\boldsymbol{k}}_{22}^* : \tilde{\boldsymbol{r}}_{22}]\, d\omega\,, \tag{4}$$

where * denotes complex conjugate and $\tilde{\boldsymbol{r}}_{ij} = \tilde{\boldsymbol{r}}(\tilde{\boldsymbol{u}}|_i, \tilde{\boldsymbol{u}}|_j)$. Thus, the dynamic stiffness of the isolator together with the generalized displacements are sufficient to describe the energy flow through the isolator. Moreover, the total energy flow is the sum of the individual energy flows through each isolator. The energy flow (4) constitutes the basic relation for the method. A closer examination of (4) shows that the real part of $\tilde{\boldsymbol{k}}_{22}$ has no influence on the energy flow, while both real and imaginary part of $\tilde{\boldsymbol{k}}_{12}$ affect the energy flow.

The number of terms in (4) is large. Moreover, the imaginary part of the driving point dynamic stiffness, i.e. $\Im\tilde{\boldsymbol{k}}_{22}$, is difficult to measure accurately under realistic conditions - high static preloads etc, due to dynamic mass loading of the test object, high cross sensitivity of force transducers, high liability to damage and poor moment transducers. However, for a vibration isolation system normally

$$\Im(\tilde{\boldsymbol{k}}_{12}^* : \tilde{\boldsymbol{r}}_{12}) \gg \Im(\tilde{\boldsymbol{k}}_{22}^* : \tilde{\boldsymbol{r}}_{22})\,, \tag{5}$$

giving

$$\langle P \rangle \approx -\frac{1}{2\pi}\int_{-\infty}^{\infty} i\omega\, \tilde{\boldsymbol{k}}_{12}^* : \tilde{\boldsymbol{r}}_{12}\, d\omega = \frac{1}{\pi}\int_{0}^{\infty} \omega\, \Im(\tilde{\boldsymbol{k}}_{12}^* : \tilde{\boldsymbol{r}}_{12})\, d\omega\,. \tag{6}$$

Reciprocity and symmetry considerations give further reductions of number of necessary terms.

Measurement of dynamic stiffness

The dynamic properties of vibration isolators are measured by an indirect method [12,13]. The test rig and measurement set up are depicted in Fig. 3, where the measurement of axial dynamic transfer stiffness is illustrated. The vibration isolator is inserted between upper and lower block. The blocks respond approximately as rigid masses, within the considered frequency range. The static preload is obtained by contracting the upper and lower block via bolts and additional vibration isolators - auxiliary resilient mountings. The static preload is measured by force gage, which is inserted between the upper auxiliary resilient mountings and upper block. The upper block is excited by two electro dynamic vibration generators. The motions of the blocks are measured by piezo electric accelerometers. The measurement set up is embedded in a rigid frame, which is constituted by a cross head, four strong columns and a heavy and rigid body. Data collection is performed by a 4-channel frequency analyzer, which also supplies the signal to the generators via an amplifier. The measurements are controlled by a PC486.

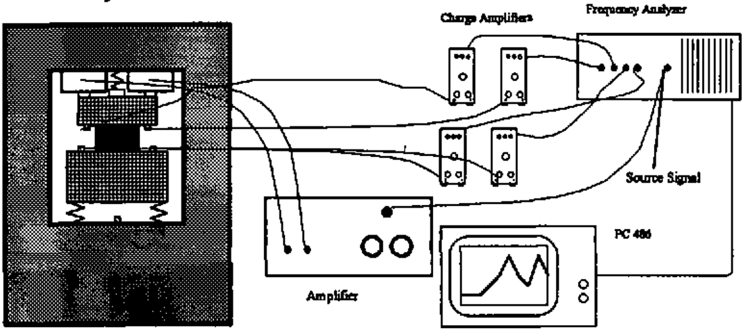

Figure 3. Test rig and measurement set up.

Briefly, the dynamic transfer stiffness is determined as follows: Let $\overset{k}{\tilde{u}}_1$ and $\overset{k}{\tilde{u}}_2$, $k = 1,2,\ldots,6$, be generalized displacement tensors at the junction to the upper and lower block, respectively. Form $\tilde{u}_1 = \overset{k}{\tilde{u}}_1 \otimes \hat{i}_k$ and $\tilde{u}_2 = \overset{k}{\tilde{u}}_2 \otimes \hat{i}_k$, where $\hat{i}_k$, $k = 1,2,\ldots,6$, are the standard basis vectors in R^6. It is possible to show that the dynamic transfer stiffness is approximately

$$\tilde{k}_{12} \approx -\omega^2 m \tilde{u}_2 \tilde{u}_1^{-1}, \tag{7}$$

where m is second order generalized mass tensor for lower block. Methods to improve the accuracy has been developed and tested. Some of the improvements are summarized below.

Improved exciting and block arrangements. A major improvement of the accuracy is achieved by exciting along one basis vector each time, see Fig. 4. In addition, the displacement vector from the mass or rotational centers of inertia of the blocks must go through the center of the junction to the isolator. This is very important for the rotational degrees of freedom, see Fig. 4.

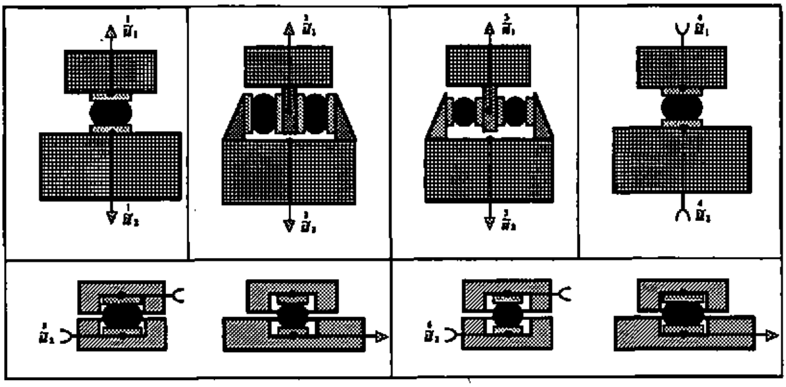

Figure 4. Improved exciting and block arrangements.

Stepped sine excitation. To increase the signal-to-noise ratio and to detect possible dynamic non-linearities, stepped sine excitation is preferable.
Effective mass. To increase the accuracy of the mass tensor for lower block, and thereby the determined dynamic stiffness, the effective mass should be used. The effective mass is determined by measurements.
Multiple load method. The accuracy is improved by identical measurements but different lower blocks. This is a form of multiple load method.
Symmetry and reciprocity technique. The dynamic transfer stiffness is symmetric due to reciprocity. In addition, vibration isolators are often geometrically symmetric. Symmetry and reciprocity are used not only to reduce the measurements but to improve the accuracy. For example, the measured vibration isolator can be inverted- 'up side down'- and measured again. The dynamic transfer stiffness is then averaged, as reciprocity implies equal dynamic transfer stiffness for both cases. Several other symmetry and reciprocity conditions can be used.
Spatial average of displacements. Several accelerometer positions close to the junction are used to 'average out' motions from other degrees of freedom.
Source correlation technique. Source correlation technique is used to reduce measurement noise. The output signal from the frequency analyzer is used as source signal.

Measurement of energy flow
The energy flow through the vibration isolators is measured indirectly. The accelerometer and experimental set up are depicted in Fig. 5. There are several aluminum cubes, which are close to the isolators and firmly bonded or bolted to the machinery or foundation. The cubes move as rigid masses. The accelerometers are attached to the cubes, generally in three perpendicular directions. Data collection is performed by 4-channel frequency analyzer. The measurements are controlled by PC486.

The static preloads for the vibration isolators are measured by force gages, which are inserted between the machinery and isolators. These force gages are not installed during the energy flow measurement.

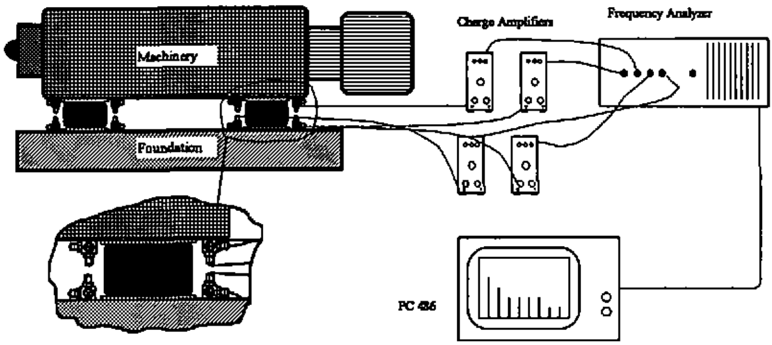

Figure 5. Energy flow measurement.

The method includes techniques to improve the accuracy, such as spatial average of displacements, signal correlation, windowing and zooming.

3. MEASUREMENT RESULTS

The developed procedure was tested for a real vibration isolation system. The energy flow from the main pump of a large hydraulic power supply unit, through four vibration isolators - Novibra C100/54A - to a steel frame was measured. The shape of the isolators is circular cylindrical. The selected vibration isolators exhibit internal anti-resonances within the considered frequency range. The dynamic transfer stiffnesses in all six degrees of freedom were measured for four preloads in the frequency range 100-1000 Hz. The results are reasonable. The rectilinear degrees of freedom were more accurately determined than the rotational degrees of freedom. Some results are shown in Fig.6.

4.CONCLUSIONS

The procedure for measurement of structure borne sound energy flow through vibration isolators works normally well, provided techniques to minimize the measurement errors are used. The main limitations are the multi point assumption, which introduces an upper frequency limit, and the inaccuracies at frequencies close to anti-resonances in the isolator and close to ranges where 'backward' energy flow through isolator occurs. Of course, strong reactive vibration fields essentially influence the measured energy flow.

5. ACKNOWLEDGEMENTS

The support of the European Economic Community; BRITE-EURAM II, contract No BRE2-CT92-0332, project No 5957, is gratefully acknowledged.

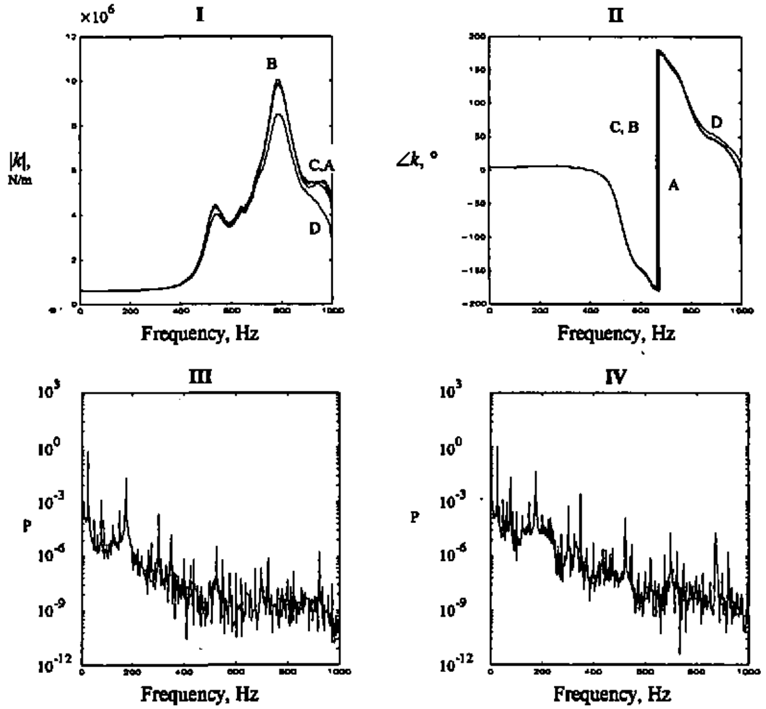

Figure 6. Magnitude(I) and phase(II) of dynamic transfer stiffness in axial direction as function of frequency. Novibra vibration isolator C100/54A, rubber hardness A. Preloads: 1375N(A), 1715N(B), 1970N(C) and 2170N(D). Normalized energy flow in axial direction through a *single* vibration isolator(III), preload 2170N, and through all vibration isolators(IV), to the foundation as function of frequency.

6. REFERENCES

[1] H.G.D. GOYDER and R.G. WHITE, *Journal of Sound and Vibration* **68**, 97-117 (1980).
[2] R.J.PINNINGTON, *Journal of Sound and Vibration* **109**, 127-139 (1986).
[3] F. JACOBSEN, *The Acoustics Laboratory, Technical University of Denmark, Report No.* 35 (1986).
[4] F. JACOBSEN and M. OHLRICH, *Proceedings, Meeting of Scandinavian Acoustical Society, Stockholm*, 281-284 (1982).
[5] R.J.PINNINGTON and R.G WHITE, *Journal of Sound and Vibration* **75**, 179-197 (1981).
[6] R.J.PINNINGTON, *Ph.D Thesis, ISVR, Southampton* (1982).
[7] R.J.PINNINGTON, *Journal of Sound and Vibration* **118**, 515-530 (1987).
[8] G. PAVIC and G. ORESKOVIC, *Proceedings, 9th International Congress on Acoustics* (1977).
[9] B. PETTERSSON and J. PLUNT, *Journal of Sound and Vibration* **82**, 517-529 (1982).
[10] B. PETTERSSON and J. PLUNT, *Journal of Sound and Vibration* **82**, 531-540 (1982).
[11] A. T. MOORHOUSE and B. M. GIBBS, *Journal of Sound and Vibration* **180**, 143-161 (1995).
[12] L. KARI, *Proceedings, 13th International Congress on Acoustics, Beograd* (1989).
[13] J. W. VERHEIJ, *Ph.D Thesis, TPD TNO-TH, Delft* (1982).